



Published in final edited form as:

Mod Pathol. 2020 August ; 33(8): 1492–1504. doi:10.1038/s41379-020-0513-4.

Myositis Ossificans-like Soft Tissue Aneurysmal Bone Cyst: A Clinical, Radiological and Pathological Study of Seven Cases with *COL1A1-USP6* fusion and a novel *ANGPTL2-USP6* fusion

Lingxin Zhang, MD^{1,4}, Sinchun Hwang, MD², Ryma Benayed, PhD¹, Guo Zhu, MD PhD⁵, Kerry A. Mullaney, MS¹, Kelly M. Rios, BS¹, Purvil Y Sukhadia, MS¹, Narasimhan Agaram, MBBS¹, Yanming Zhang, MD¹, Julia A. Bridge, MD^{6,7}, John H. Healey, MD³, Edward A. Athanasian, MD³, Meera Hameed, MD¹

¹Department of Pathology, Memorial Sloan Kettering Cancer Center, New York, NY, 10065

²Department of Radiology, Memorial Sloan Kettering Cancer Center, New York, NY, 10065

³Department of Orthopedic Surgery, Memorial Sloan Kettering Cancer Center, New York, NY, 10065

⁴Department of Pathology and Laboratory Medicine, Hospital for Special Surgery, New York, NY, 10021

⁵Department of Pathology, Cooper University Health Care, Camden, NJ, 08103

⁶Department of Pathology and Microbiology, University of Nebraska Medical Center, Omaha, NE, 68198

⁷Division of Molecular Pathology, The Translational Genomics Research Institute, Phoenix, AZ 85004

Abstract

Herein we described the clinical, radiological, histological and molecular characteristics of seven soft tissue aneurysmal bone cyst (STABC) diagnosed and managed at a tertiary cancer center and to elucidate its relationship with myositis ossificans (MO). All cases had established imaging and histopathological diagnosis of STABC and were subject to fluorescent *in situ* hybridization (FISH) for *USP6* rearrangement and Archer® FusionPlex® targeted RNA sequencing analysis (RNASeq) to identify the fusion partner. A thorough literature review of STABC and MO was conducted. The patients presented with painful masses unprecedented by trauma, occurring most commonly in the deep soft tissue of the thigh/gluteus (4/7), and also in the supraclavicular region, the axilla, and the hand. On imaging, the lesions were frequently associated with peripheral calcification on conventional radiographs and CT (6/7), cystic components on ultrasound and MRI, as well as perilesional edema (7/7) and fluid levels (3/7) on MRI. Bone scan (1/1) showed intense radiotracer uptake. Histologically, 6/7 cases demonstrated zonal arrangements reminiscent of MO. *USP6*

Correspondence: Meera Hameed MD, Memorial Sloan Kettering Cancer Center, Department of Pathology, Address: 1275 York Ave., New York, NY 10065, Phone: (212) 639-8225, hameedm@mskcc.org.

Disclosure/Conflict of Interest

The authors do not have conflicts of interest to disclose.

rearrangement was found in all seven cases by FISH and/or RNASeq. RNASeq further detected *COL1A1-USP6* fusion in six cases and a novel *ANGPTL2-USP6* fusion in one case. Four patients underwent resection of the tumors and were disease-free at their last follow-up. Three patients who underwent incisional or needle biopsies had no evidence of disease progression on imaging studies. In conclusion, the clinical, radiological and pathological overlap between STABC and MO suggests that they are closely related entities. A novel fusion *ANGPTL2-USP6* is associated with distinct clinical and pathological presentation.

Keywords

Myositis Ossificans-like Soft Tissue Aneurysmal Bone Cyst (MO-like STABC); *USP6*; *COL1A1*; *ANGPTL2*; CT; MRI; Radiograph

Introduction

Although primary aneurysmal bone cyst (ABC) of bone was originally thought to be reactive when the entity was recognized by Jaffe and Lichtenstein in 1942¹, evidence suggesting its neoplastic nature was established when Panoutsakopoulos and colleagues² discovered a recurrent chromosome aberration, t(16;17)(q22;p13). This was subsequently proven by Oliveira and colleagues to result in a fusion gene in which the promoter region of the osteoblast cadherin 11 gene (*CDH11*) at 16q22 is fused to the entire ubiquitin-specific protease 6 (*USP6*; alias *Tre2*) coding sequence at 17p13, transcriptionally upregulating the latter^{3,4}. Alternative 5' fusion partners to *USP6* gene—*THRAP3* (1p34.3), *FOSL2* (2p23.2), *CTNNB1* (3p22.1), *CNBP* (3q21.3), *SEC31A* (4q21.22), *SPARC* (5q33.1), *OMD* (9q22.31), *PAFAH1B1* (17p13.3), *COL1A1* (17q21.33), *EIF1* (17q21.2), *STAT3* (17q21.2) and *USP9X* (Xp11)—have been subsequently described^{5–9}, whereas *CDH11* remains the most common fusion partner in primary ABCs of bone.

Oliveira and colleagues tested for *USP6* rearrangements in morphological mimickers of primary ABCs such as secondary ABCs, myositis ossificans (MO), brown tumor, and cherubism, and found *USP6* rearrangements in 2 of 12 cases with classic radiological and histological features of MO¹⁰. Recently, MO-like lesions with *USP6* rearrangement were reported under both terms of MO^{11,12} and STABC¹³. The discordance in nomenclature in part reflects the overlapping radiological and pathological features of these newly defined *USP6* rearranged lesions with MO and primary bone ABC. Our cases herein referred to as MO-like STABCs emphasize this diagnostic challenge with detailed case examples and the value of molecular analysis for diagnostic confirmation. The objective of this study is two-fold — (1) to describe the clinical course, radiological characteristics, and histological features of MO-like STABC; (2) and to identify the fusion partners for *USP6* by targeted RNA sequencing (RNASeq).

Material and Methods

The study was conducted at a tertiary cancer center with approval by the Institutional Review Board (protocol# 18-215).

Eight patients with MO-like STABCs diagnosed between 2009 and 2018 were identified by searching the pathology laboratory information system. Hematoxylin and Eosin (H&E) stained slides from archival formalin-fixed paraffin-embedded (FFPE) blocks were reviewed and radio-pathological correlation was performed. Specimens with sufficient tumor content (>10%) that were not subjected to acid decalcification were submitted for molecular studies.

Fluorescence *in Situ* Hybridization (FISH) Analysis for *USP6* Rearrangement

FFPE tissue samples were tested for *USP6* rearrangements by a break-apart fluorescence *in situ* hybridization (FISH) assay using a commercial *USP6* break-apart FISH probe (Zytovision 27572 Bremerhaven Germany). FFPE tissue sections (4 mm thick) generated from FFPE blocks of tumor specimens were pretreated by deparaffinization in xylene and dehydration in ethanol. Dual-color FISH assay was conducted according to the protocol for FFPE sections from Vysis/Abbott Molecular with a few modifications. FISH analysis and signal capture were conducted on a fluorescence microscope (Zeiss, Jena, Germany) coupled with ISIS FISH Imaging System (Metasystems, Altlußheim, Germany). We analyzed 100 interphase nuclei from each tumor specimen, except for case 7, in which 50 interphase nuclei were analyzed due to regional suboptimal signal quality.

RNA Extraction and Targeted Sequencing

A minimum of 10 unstained slides were subject to deparaffinization. RNA extraction was then performed using RNeasy FFPE Kit according to the manufacturer's protocol (Qiagen, Catalog #73504). cDNA libraries were constructed according to the Archer FusionPlex™ protocol (previously described by Zheng et al.¹⁴) with manufacturer supplied reagents including Archer® Universal RNA Reagent Kit for Illumina® (Catalog #AK-0040-8), Archer MBC adapters (Catalog #SA0040-45) and custom designed Gene Specific Primer (GSP) Pool kit. A total 346 fusion unidirectional GSPs, ranging in length from 18 to 39 base pairs, have been designed to target specific exons in 62 genes known to undergo rearrangement in tumorigenesis based on current literature¹⁵. GSPs are hybridized in either 5'-to-3' or 3'-to-5' direction to the relevant exons of each gene in order to enrich the cDNA libraries for known and novel fusion transcripts in combination with adapter-specific primers. The enriched amplicons were sequenced on an Illumina MiSeq instrument. A high confidence fusion event was reported when supported by a minimum of 5 breakpoint-spanning unique reads and 3 breakpoint-spanning reads with unique start sites.

Results

Clinical, radiological and pathological features

Of the 8 MO-like STABCs, one case showed *USP6* rearrangement by FISH but was excluded from the study due to insufficient material for RNASeq.

The remaining 7 patients included 5 females and 2 males with a median age of 32 years (14 to 51 years). All patients presented with a painful mass without antecedent trauma. Two patients (cases 3 and 5) had symptoms for more than 6 months. These lesions ranged from 2.4 cm to 6.0 cm in greatest dimension and were located in the thigh/gluteus (4), supraclavicular region (1), axilla (1), and hand (1). Two lesions were juxtacortical (cases 2

and 6). All patients underwent imaging studies. Four lesions were solid (4/7), while others were partially cystic with fluid levels (3/7) on ultrasound and/or MRI. Peripheral calcifications were typically seen on plain radiograph and CT (5/7) at initial presentation, which increased over the course. On MRI, the lesions exhibited perilesional edema (7/7) with enhancement. Bone scan (1/1) showed intense radiotracer uptake, which markedly decreased at a follow-up bone scan. Histologically, 6/7 cases (except for case 3) had zonal growth pattern seen in classic MO, composed of (myo)fibroblastic spindle cells, multinucleated giant cells and blood-filled sinusoids in the center, in most cases confined by reactive woven bone at the periphery, while the lesion in case 3 was infiltrative with clustered calcification. FISH study in 6/7 cases showed rearrangement of *USP6* with either split of the 5' and 3' signals or a single 3' signal. Subsequent RNASeq detected *USP6* rearrangement in all 7 cases. In 6/7 cases RNASeq showed a *COL1A1-USP6* fusion. Case 3 had a novel *ANGPTL2-USP6* fusion. In all cases, the breakpoints were located in exon 1 of *USP6*, placing the entire coding sequence of *USP6* under the influence of the promoter region of *COL1A1* and most likely promoter region of *ANGPTL2* in case 3. (see Figure 1). Six patients (except for patient 4) were followed for a median of 26.5 months. Patient 3 underwent resection after having persistent symptoms for about 3.5 years. The remaining patients had resolved symptoms following resection or biopsy. The clinical, radiological, and pathological findings of all cases are summarized in detail in Table 1.

Case 1

A 32-year-old woman presented with an enlarging, painful mass in her left proximal thigh for 2 months (Figure 2). Imaging studies showed a partially cystic mass without calcification. Although the clinical and imaging presentations were suggestive of a nodular fasciitis, the clinical course was not typical. A wide resection of the mass was performed. Grossly, the mass had a thick, ossified wall and a central cystic space with hemorrhage. Microscopic examination showed a lesion with zonal phenomenon. The inner cystic areas were lined by fibroblast-like spindle cells and occasional osteoclast-like giant cells and background inflammatory cells, reminiscent of ABC. In the middle zone, osteoid was being laid down by the proliferating spindle cells, which gradually merged into the outer zone of trabeculated, osteoblast-rimmed woven bone, focally containing cartilage. The patient remained disease-free 3.5 years postoperatively.

Case 2

A 17-year-old young man noted a painful, palpable mass in his left clavicle for 6 weeks. The radiological differential diagnoses included infection, intracortical osteoid osteoma, periosteal osteoblastoma, and STABC. The lesion was resected along with the periosteum. The macro- and microscopic findings were similar to those in case 1. There was no recurrence five months after the resection.

Case 3

A 46-year-old woman noticed a mass in her left gluteus/thigh that caused soreness (Figure 3). On imaging studies, the mass continued to grow over 6 months from 5.1 cm to 6.0 cm. Clinical and radiological differential diagnoses included deep fibromatosis (desmoid tumor), nodular fasciitis, and MO. Biopsy showed fibroblastic spindle cell proliferation in a

collagenized stroma. The cellularity was variable but in general low. Osteoclast-like giant cells were focally scattered around osteoid. No blood-filled cysts or reactive bone trabeculae were seen. The mass was resected 3.5 years after the initial presentation given the patient's persistent symptoms. Gross examination showed a $7.5 \times 4.2 \times 2.9$ cm predominantly solid, ill-defined, and lobulated mass with multifocal ossification involving the deep adipose tissue and skeletal muscle. Histologic sections showed fibroblastic proliferation that was previously seen on the biopsy infiltrating into adipose tissue with multiple haphazard foci of reactive woven bone.

Case 4

A 51-year-old woman suddenly noticed a tender lump in the hypothenar region of the left hand. A needle biopsy showed a solid fibroblastic proliferation in a loose stroma alternating with dense collagen bundles (osteoid), reminiscent of an early MO. After 3 months, the mass was extricated displaying a vague zonal pattern with markedly decreased cellularity in the center and mineralized collagen matrix at the periphery. The patient was lost to follow-up.

Case 5

A 22-year-old woman presented with left shoulder pain for 6 months. Although the main consideration radiologically was a MO, the anatomic site and protracted clinical course were rather unusual.

An open biopsy showed elements reminiscent of a MO, including fibroblastic spindle cell proliferation, osteoclast-like giant cells centered around blood-filled sinusoids, and osteoblast-rimmed woven bone maturing into lamellar bone. A resection was not performed given the proximity of the lesion to the brachial plexus and axillary vessels. The patient reported significantly improved range of motion after the open biopsy, and her axillary mass had decreased in size and residual dense calcification and remained stable at 4.5-year post-operative follow-up.

Case 6

A 14-year-old girl, an avid dancer, developed sudden pain in her right thigh 3 weeks prior to presentation (Figure 4). The pain limited her mobility and was inadequately relieved by anti-inflammatory medication. Imaging studies showed a solid, calcified lesion in the vastus intermedius muscle, with associated right femoral diaphyseal periosteal reaction and intense radiotracer uptake, raising concern for a surface osteosarcoma. No intracortical lesion was identified. Radiological differential diagnoses were broad, including solid ABC, bizarre parosteal osteochondromatous proliferation, and MO. Bone tumors such as Ewing sarcoma, osteosarcoma, or osteoblastoma were also considered. An incisional biopsy showed a solid lesion with exuberant interconnecting woven bone, favoring a benign etiology. The bony matrix was embedded within a collagenized to myxoid stroma with variably cellular fibroblastic spindle cells and thick-walled vessels. Occasional osteoclast-like giant cells were also identified, however, without associated blood-filled sinusoids. The patient was asymptomatic at the last follow-up.

Case 7

A 42-year-old man developed subacute right thigh pain and swelling. Main differential diagnoses based on imaging findings included MO and solid ABC. A needle biopsy demonstrated similar findings as those in case 5. In 3 months, the mass decreased in size and the patient's associated pain resolved.

Discussion

Historically, “myositis ossificans”, also known as myositis ossificans circumscripta and myositis ossificans traumatica, is localized and self-limiting. The condition affects individuals of any age with a male predominance but is most commonly documented in adolescents and athletically active young adults. It is commonly agreed that trauma (e.g. stab wound, blunt trauma) or repetitive mechanical stress (e.g. “rider’s bone,” “fencer’s bone”) is the initiating event in most cases, while arthroplasty, fractures, spinal cord damage and thermal injury are also risk factors^{16,17}. It usually presents as a localized mass, but occasionally can be infiltrative. Within a few days of trauma, radiographs show a rounded discrete soft tissue swelling. It takes about six weeks before ossifications at the periphery becomes apparent on radiography. In about two months, MO reaches its maximal size and definitive outline, then continues to mature and ossify in 5 to 6 months. Although the condition is not rare, the pathogenesis of MO has not been well elucidated. Earlier authors placed MO in a middle ground between inflammatory process and a neoplasm, while some pathologists favor it to be a true neoplasm^{16,18,19}. Undoubtedly MO is a benign process and may involute over time, therefore can be conservatively managed. But it may present to the pathologist as a pseudosarcomatous soft tissue tumor, particularly during its rapidly developing phase and when it arises in the juxta-cortical location, radiographically mimicking osteochondroma or osteosarcoma (as in case 6). If biopsied, the histology may display a highly cellular osteoblastic proliferation with osteoid or woven bone formation. However, MO has a characteristic “zonal phenomenon,” composed of a well-delimited outer rim of bony spicules, a central area of proliferating fibroblastic spindle cells with multinuclear giant cells, and a transition zone of osteoblasts with islands of immature bone. The circumscription with zonation usually separates MO from the more ominous infiltrating surface osteosarcomas however deceptively benign the cytology the latter may show.

In 1992, Amir et al.²⁰ reported a MO that spontaneously occurred in a 15-year-old girl, which contained a central radiolucent area made up of multiple blood-filled, cyst-like spaces. This lesion was interpreted as MO with ABC changes. Following this report, Rodríguez-Peralto et al.²¹ first used the term “primary aneurysmal cyst of soft tissues” in describing a MO-like lesion with histological features identical to those found in ABC of bone. More STABCs were described in the literature and almost all of them had overlapping clinical and radiological features of MO^{10,12,13,22–31}(Table 2). As with MO, STABC affects patients with a wide age distribution (6-62, mean age 30 years) without gender predilection and presents as a painful, rapidly enlarging mass. The thigh, gluteus, upper arm, shoulder and axilla are most commonly affected regions. Although in previous reports cystic components were common on imaging studies^{13,25}, fluid-fluid levels on MRI were only present in 3/7 (43%) of our cases, which may be explained by different temporal stages. In

the current standard care for MO-like lesions, a biopsy is only performed when the clinical presentation deviates from a classic MO, making watchful waiting clinically untenable. Thus there is a selection bias in STABC and therefore, suggested clinical and radiological features to differentiate STABC from MO such as lack of perceived trauma and protracted clinical course are not entirely specific.

FISH and RNASeq studies for *USP6* (chromosome 17p13.2) rearrangement in STABC^{5,10,13,27,28,31} have proved to be objective tools for diagnosis. The lesions in our series encompassed a variety of anatomic sites (e.g. axilla, tendon insertion site), beyond the intramuscular locations of classic MO. Still, the overlapping clinical, radiological and pathological features between STABCs and MOs suggest that they are closely related entities. Indeed, Bekers et al. stated that MO is another “transient neoplasm” characterized by recurrent rearrangement of *USP6*, a promiscuous fusion partner identified in primary ABC of bone, nodular fasciitis^{32,33}, cellular fibroma of tendon sheath³⁴, giant cell rich lesions of the small bones³⁵ and more recently in cranial fasciitis^{36,37} and fibro-osseous pseudotumor of digits^{12,38} (Table 3).

While primary ABC of bone demonstrates variant translocations with multiple partners, the fusion partners for STABC has remained relatively consistent with *COL1A1*^{5,13,31}. *COL1A1* encodes for the collagen alpha 1 polypeptide chain and mutations in the gene are associated with many inherited disorders such as osteogenesis imperfecta, Ehlers-Danlos syndrome, infantile cortical hyperostosis, and idiopathic osteoporosis³⁹. In the neoplastic setting, this gene is well known for this diagnostic fusion with the platelet-derived growth factor B-chain (*PDGFB*) gene in dermatofibrosarcoma protuberans and giant cell fibroblastoma driving the constitutive activation of *PDGFB* gene⁴⁰. *COL1A1* is mapped to 17q21-17q22, with opposite orientation with *USP6* at 17p13. Previous cytogenetic with subsequent RNA sequencing studies^{25,31} in two STABCs showed *COL1A1-USP6* fusion involving exon 1 of *COL1A1* and a splicing variant of *USP6* exon 1 or exon 2. The RNASeq results in 6 of our cases showed consistent breakpoints in exon 1 of *COL1A1* and *USP6* exon 1.

Case 3 was unique for the lack of zonal growth pattern and a novel *ANGPTL2-USP6* fusion. *ANGPTL2* (angiopoietin related protein-2) at 9q33 is a member of vascular endothelial growth factor family, known not only for its angiogenic and antiapoptotic properties but also for its pro-inflammatory properties⁴². In our case, the fusion involved exon 1 of *ANGPTL2* and the entire coding sequence of *USP6*. It is likely that *ANGPTL2* also contributes with its promoter. It is unknown how these fusions recapitulate similar pathological processes within bone and soft tissue.

Oliveira and colleagues⁴³ studied the molecular pathogenesis underlying the role of *USP6* in ABCs and showed that *USP6* residing in the fibrous stromal component of ABC induces transcription of matrix metalloproteinase (MMP) through activation of the nuclear factor κ B (NF κ B), which seems to play a role in matrix degradation, angiogenesis, and inflammatory response. More recently, an essential mediator of *USP6*'s pathogenic mechanism has been recognized as the *Jak1-STAT3* pathway⁴⁴, which act in concert with NF κ B. This biological effect explains the histological features of the lesion mimicking a reparative/reactive hemorrhagic process and thus the long-term assumption that ABC was non-neoplastic albeit

this was a destructive lesion of the bone. While the cell line of differentiation remains elusive, most of the reported fusion partners of ABC of bone are expressed during osteoblastic differentiation and it is suggested that the neoplastic cell could be derived from osteoblasts⁵. A common breakpoint is in exon 1 or 2 of the 5' partner gene, which fuses with the first coding exon of *USP6*; the expected functional consequence being upregulated expression of an intact USP6 protein under the influence of the highly active promoter of the partner gene^{5,45}.

In conclusion, MO-like STABC is a benign neoplasm with *USP6* rearrangement, characterized with overlapping histological features with MO and primary bone ABC. Thigh, upper arm, and shoulder are common locations. Peripheral calcification on plain radiograph and CT, perilesional edema, and fluid-fluid levels on MRI are frequently observed radiological features. En-bloc excision is curative when the lesions cause symptoms. Majority of cases show *COL1A1-USP6* fusion and herein we have described an additional case with *ANGPTL2* gene as a novel fusion partner with *USP6*.

Acknowledgements:

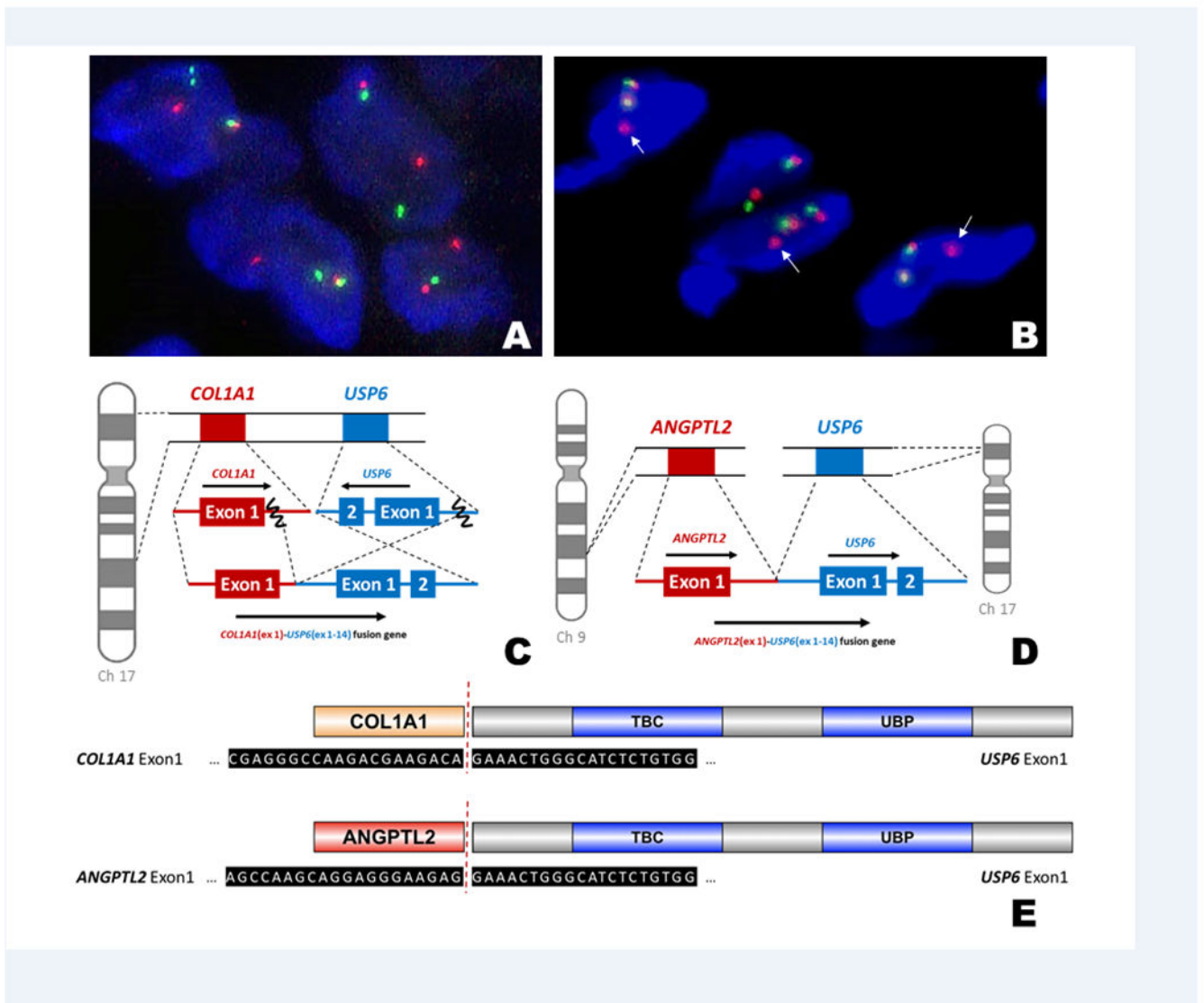
The authors declare that they have no conflict of interest. This work was supported by the Department of Pathology at Memorial Sloan Kettering Cancer Center Internal Research Fund, and in part by a National Institutes of Health/ National Cancer Institute Cancer Center Support Grant under award P30CA008748. The content is solely the responsibility of the authors and does not necessarily represent the official views of the National Institutes of Health. This study was presented in part at the Association of Molecular Pathology 2018 Annual Meeting, November 1, 2018, San Antonio, Texas, USA.

References

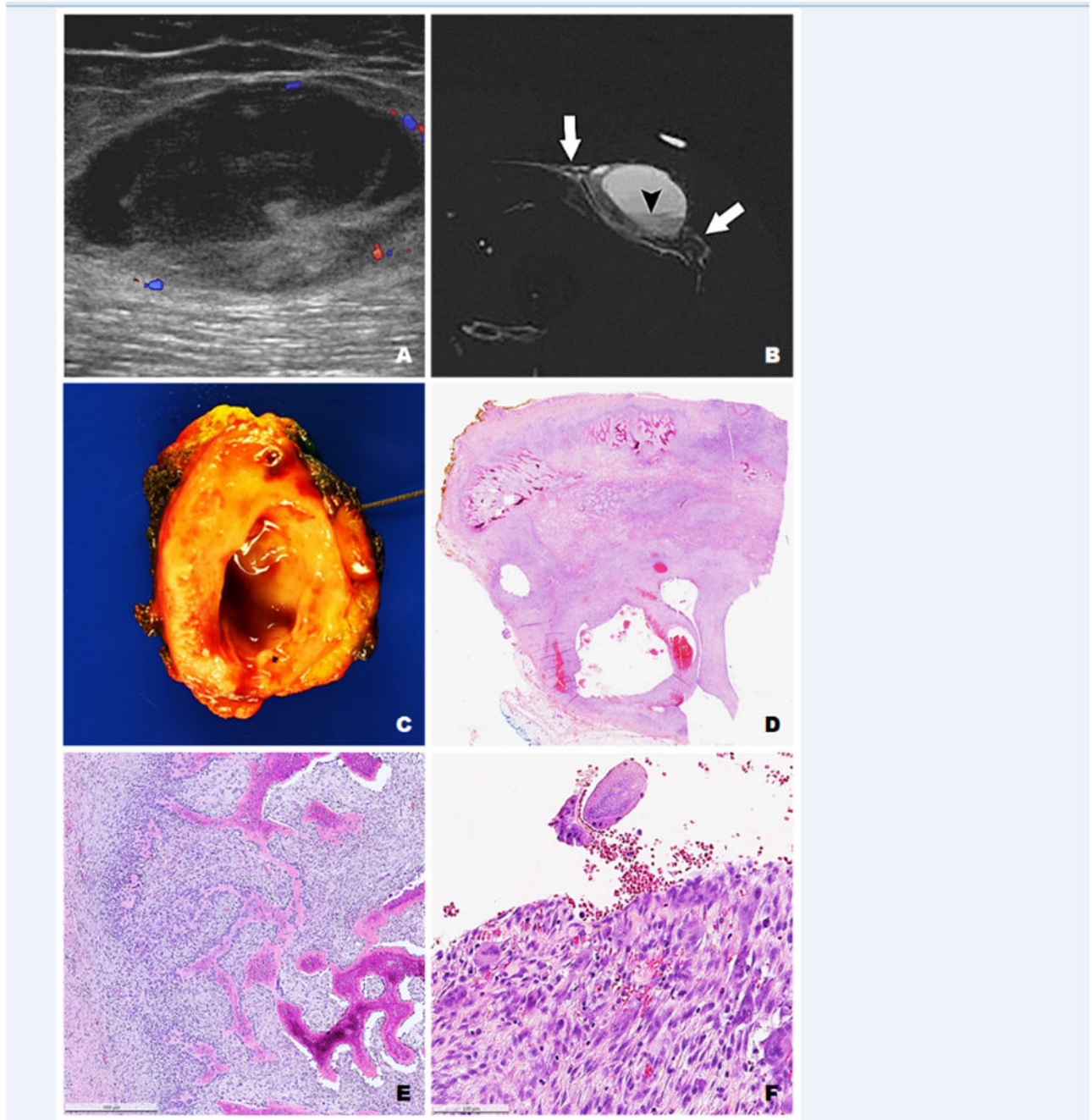
1. Jaffe HL, Lichtenstein L. Solitary unicameral bone cyst: with emphysema on the roentgen picture, the pathologic appearance and the pathogenesis. *Arch Surg* 1942;44:1004–1025.
2. Panoutsakopoulos G, Pandis N, Kyriazoglou I, Gustafson P, Mertens F, Mandahl N. Recurrent t(16;17)(q22;p13) in aneurysmal bone cysts. *Genes Chromosomes Cancer* 1999;26:265–266. [PubMed: 10502326]
3. Oliveira AM, Hsi BL, Weremowicz S. USP6 (Tre2) Fusion Oncogenes in Aneurysmal Bone Cyst. *Cancer Res* 2004;64:1920–1923. [PubMed: 15026324]
4. Oliveira AM, Perez-Atayde AR, Inwards CY, Medeiros F, Derr V, Hsi BL et al. USP6 and CDH11 Oncogenes Identify the Neoplastic Cell in Primary Aneurysmal Bone Cysts and Are Absent in So-Called Secondary Aneurysmal Bone Cysts. *Am J Pathol* 2004;165:1773–1780. [PubMed: 15509545]
5. Oliveira AM, Perez-Atayde AR, Dal Cin P, Gebhardt MC, Chen CJ, Neff JR, et al. Aneurysmal bone cyst variant translocations upregulate USP6 transcription by promoter swapping with the ZNF9, COL1A1, TRAP150 and OMD genes. *Oncogene* 2005;24:3419–3426. [PubMed: 15735689]
6. Panagopoulos I, Mertens F, Löfvenberg R, Mandahl N. Fusion of the COL1A1 and USP6 genes in a benign bone tumor. *Cancer Genet Cytogenet* 2008;180:70–73. [PubMed: 18068538]
7. Guseva NV, Jaber O, Tanas MR, Stence AA, Sompallae R, Schade J, et al. Anchored multiplex PCR for targeted next-generation sequencing reveals recurrent and novel USP6 fusions and upregulation of USP6 expression in aneurysmal bone cyst. *Genes Chromosomes Cancer* 2017;56:266–277. [PubMed: 27910166]
8. Šekoranja D, Boštjan i E, Salapura V, Mav i B, Pižem J. Primary aneurysmal bone cyst with a novel SPARC-USP6 translocation identified by next-generation sequencing. *Cancer Genet* 2018;228–229:12–16.

9. Blackburn PR, Davila JI, Jackson RA, Fadra N, Atiq MA, Pitel BA, et al. RNA sequencing identifies a novel USP9X-USP6 promoter swap gene fusion in a primary aneurysmal bone cyst. *Genes Chromosomes Cancer* 2019;58:589–594. [PubMed: 30767316]
10. Sukov WR, Franco MF, Erickson-Johnson M, Chou MM, Unni KK, Wenger DE, et al. Frequency of USP6 rearrangements in myositis ossificans, brown tumor, and cherubism: molecular cytogenetic evidence that a subset of “myositis ossificans-like lesions” are the early phases in the formation of soft-tissue aneurysmal bone cyst. *Skeletal Radiol* 2008;37:321–327. [PubMed: 18265974]
11. Bekers EM, Eijkelenboom A, Grünberg K, Roverts RC, de Rooy JW, van der Geest IC, et al. Myositis ossificans – Another condition with USP6 rearrangement, providing evidence of a relationship with nodular fasciitis and aneurysmal bone cyst. *Ann Diagn Pathol* 2018;34:56–59. [PubMed: 29661729]
12. Švajdler M, Michal M, Martínek P, Ptáková N, Kinkor Z, Szépe P, et al. Fibro-osseous pseudotumor of digits and myositis ossificans show consistent COL1A1-USP6 rearrangement: a clinicopathological and genetic study of 27 cases. *Hum Pathol* 2019;88:39–47. [PubMed: 30946936]
13. Song W, Suurmeijer AJH, Bollen SM, Cleton-Jansen AM, Bovée JV, Kroon HM. Soft tissue aneurysmal bone cyst: six new cases with imaging details, molecular pathology, and review of the literature. *Skeletal Radiol* 2019;48:1059–1067. [PubMed: 30603771]
14. Zheng Z, Liebers M, Zhelyazkova B, Cao Y, Panditi D, Lynch KD, et al. Anchored multiplex PCR for targeted next-generation sequencing. *Nat Med* 2014;20:1479–1484. [PubMed: 25384085]
15. Zhu G, Benayed R, Ho C, Mullaney K, Sukhadia P, Rios K, et al. Diagnosis of known sarcoma fusions and novel fusion partners by targeted RNA sequencing with identification of a recurrent ACTB-FOSB fusion in pseudomyogenic hemangioendothelioma. *Mod Pathol* 2019;32:609. [PubMed: 30459475]
16. Ackerman LV. Extra-osseous localized non-neoplastic bone and cartilage formation (so-called myositis ossificans): clinical and pathological confusion with malignant neoplasms. *J Bone Joint Surg Am* 1958;40-A:279–298. [PubMed: 13539055]
17. Meyers C, Lisiecki J, Miller S, Levin A, Fayad L, Ding C, et al. Heterotopic Ossification: A Comprehensive Review. *JBMR Plus* 2019;3:e10172. [PubMed: 31044187]
18. Binnie JF XIII. Myositis Ossificans Traumatica. *Ann Surg* 1903;38:423–440. [PubMed: 17861354]
19. Gruca A Myositis ossificans circumscripta: A clinical and experimental study. *Ann Surg* 1925;82:883–919. [PubMed: 17865374]
20. Amir G, Mogle P, Sucher E. Case report 729. Myositis ossificans and aneurysmal bone cyst. *Skeletal Radiol* 1992;21:257–259. [PubMed: 1626294]
21. Rodríguez-Peralto JL, López-Barea F, Sánchez-Herrera S, Atienza M, et al. Primary aneurysmal cyst of soft tissues (extraosseous aneurysmal cyst). *Am J Surg Pathol* 1994;18:632–636. [PubMed: 8179078]
22. Lopez-Barea F, Burgos-Lizalde E, Rodríguez-Peralto JL, Alvarez-Linera J, Sanchez-Herrera S. Primary aneurysmal cyst of soft tissue: Report of a case with ultrastructural and MRI studies. *Virchows Arch* 1996;428:125–129. [PubMed: 8925126]
23. Shannon P, Bedard Y, Bell R, Kandel R. Aneurysmal cyst of soft tissue: Report of a case with serial magnetic resonance imaging and biopsy. *Hum Pathol* 1997;28:255–257. [PubMed: 9023413]
24. Nielsen GP, Smith MA, Rosenberg AE. Soft Tissue Aneurysmal Bone Cyst. *Am J Surg Pathol* 2002;26:6.
25. Wang XL, Gielen JL, Salgado R, Delrue F, De Schepper AMA. Soft tissue aneurysmal bone cyst. *Skeletal Radiol* 2004;33:477–480. [PubMed: 15150676]
26. Ajillogba KA, Kaur H, Duncan R, McFarlane JH, Watt AJ. Extraosseous aneurysmal bone cyst in a 12-year-old girl. *Pediatr Radiol* 2005;35:1240–1242. [PubMed: 16172893]
27. Ellison DA, Sawyer JR, Parham DM, Nicholas R Jr Soft-Tissue Aneurysmal Bone Cyst: Report of a Case with t(5;17)(q33;p13). *Pediatr Dev Pathol* 2007;10:46–49. [PubMed: 17378626]
28. Pietschmann MF, Oliveira AM, Chou MM, Ihrler S, Niederhagen M, Baur-Melnyk A, et al. Aneurysmal Bone Cysts of Soft Tissue Represent True Neoplasms: A Report of Two Cases. *J Bone Jt Surg-Am Vol* 2011;93:e45-1–8.

29. Hao Y, Wang L, Yan M, Jin F, Ge S, Dai K. Soft tissue aneurysmal bone cyst in a 10-year-old girl. *Oncol Lett* 2012;3:545–548. [PubMed: 22740948]
30. Baker KS, Gould ES, Patel HB, Hwang SJ. Soft tissue aneurysmal bone cyst: a rare case in a middle aged patient. *J Radiol Case Rep* 2015;9. doi:10.3941/jrcr.v9i1.2157.
31. Jacquot C, Szymanska J, Nemana LJ, Steinbach LS, Horvai AE. Soft-tissue aneurysmal bone cyst with translocation t(17;17)(p13;q21) corresponding to COL1A1 and USP6 loci. *Skeletal Radiol* 2015;44:1695–1699. [PubMed: 26142538]
32. Erickson-Johnson MR, Chou MM, Evers BR, Roth CW, Seys AR, Jin L, et al. Nodular fasciitis: a novel model of transient neoplasia induced by *MYH9-USP6* gene fusion. *Lab Invest* 2011;91:1427–1433. [PubMed: 21826056]
33. Patel NR, Chrisinger JSA, Demicco EG, Sarabia SF, Reuther J, Kumar E, et al. USP6 activation in nodular fasciitis by promoter-swapping gene fusions. *Mod Pathol* 2017;30:1577–1588. [PubMed: 28752842]
34. Carter JM, Wang X, Dong J, Westendorf J, Chou MM, Oliveira AM. USP6 genetic rearrangements in cellular fibroma of tendon sheath. *Mod Pathol* 2016;29:865–869. [PubMed: 27125357]
35. Agaram NP, LeLoarer FV, Zhang L, Hwang S, Athanasian EA, Hameed M, et al. USP6 gene rearrangements occur preferentially in giant cell reparative granulomas of the hands and feet but not in gnathic location. *Hum Pathol* 2014;45:1147–1152. [PubMed: 24742829]
36. Yancoskie A, Stojanov I, Fantasia J, Edelman M. USP6 Gene Rearrangement in Cranial Fasciitis: A Report of Three Cases. *Oral Surg Oral Med Oral Pathol Oral Radiol* 2017;124:e222.
37. Paulson VA, Stojanov IA, Wasman JK, Restrepo T, Cano S, Plunkitt J, et al. Recurrent and novel USP6 fusions in cranial fasciitis identified by targeted RNA sequencing. *Mod Pathol* 2019:1–6.
38. Flucke U, Shepard SJ, Bekers EM, Tirabosco R, van Diest PJ, Creytens D, et al. Fibro-osseous pseudotumor of digits-Expanding the spectrum of clonal transient neoplasms harboring USP6 rearrangement. *Ann Diagn Pathol* 2018;35:53–55. [PubMed: 29787930]
39. Online Mendelian Inheritance in Man, OMIM (TM). MIM #120150. 2018. Available from: <http://www.ncbi.nlm.nih.gov/omim>.
40. Simon MP, Pedeutour F, Sirvent N, Grosgeorge J, Minoletti F, Coindre JM, et al. Deregulation of the platelet-derived growth factor B-chain gene via fusion with collagen gene COL1A1 in dermatofibrosarcoma protuberans and giant-cell fibroblastoma. *Nat Genet* 1997;15:95–98. [PubMed: 8988177]
41. Althof PA, Ohmori K, Zhou M, Bailey JM, Bridge RS, Nelson M, et al. Cytogenetic and molecular cytogenetic findings in 43 aneurysmal bone cysts: aberrations of 17p mapped to 17p13.2 by fluorescence *in situ* hybridization. *Mod Pathol* 2004;17:518–525. [PubMed: 15044915]
42. Thorin-Trescases N, Thorin E. Angiopoietin-like-2: a multifaceted protein with physiological and pathophysiological properties. *Expert Rev Mol Med* 2014;16:e17. [PubMed: 25417860]
43. Oliveira AM, Chou MM. The TRE17/USP6 oncogene: a riddle wrapped in a mystery inside an enigma. *Front Biosci Sch Ed* 2012;4:321–334.
44. Quick L, Young R, Henrich IC, Wang X, Asmann YW, Oliveira AM, et al. Jak1–STAT3 Signals Are Essential Effectors of the USP6/TRE17 Oncogene in Tumorigenesis. *Cancer Res* 2016;76:5337–5347. [PubMed: 27440725]
45. Oliveira AM, Chou MM. USP6-induced neoplasms: the biologic spectrum of aneurysmal bone cyst and nodular fasciitis. *Hum Pathol* 2014;45:1–11. [PubMed: 23769422]

**FIGURE 1.**

(A) Fluorescence *in situ* hybridization (FISH) analysis with break-apart probes flanking the *USP6* gene (5' – green, 3' – orange) showed a split of the green and orange signals, indicating disruption of *USP6*. (B) Two normal signals and a single 3' (arrow) signal indicative of *USP6* gene rearrangement was seen in case 3. (C) This schematic diagram represents the most common fusion pattern in our series of MO-like ABCs (6/7 cases), with breakpoints within exon 1 of *COL1A1* (17q21-1722) and exon 1 of *USP6* (17p13). (D) A novel fusion between *ANGPTL2* (9q33) and *USP6* was found in case 3. (E) The *COL1A1*-*USP6* and *ANGPTL2*-*USP6* fusion products included the promoter region of the *COL1A1* and *ANGPTL2* and the entire coding sequence of *USP6*.

**FIGURE 2.**

Case 1 - (A) A longitudinal ultrasound image of the anterior thigh showed a partially cystic subcutaneous mass with irregular rim and peripheral vascular flow. **(B)** On axial T2 weighted MR image, the mass had high signal with thickened rim and fluid level (arrowhead). It compressed on and infiltrated the adjacent fascia (arrows). **(C)** The excised mass had a tan-white, glistening and firm cut surface with a central cystic space with hemorrhage. **(D)** The lesion displayed a MO-like zonal pattern composed of an outer shell of reactive woven bone with a hypocellular stroma **(E)** and central blood-filled cysts lined by

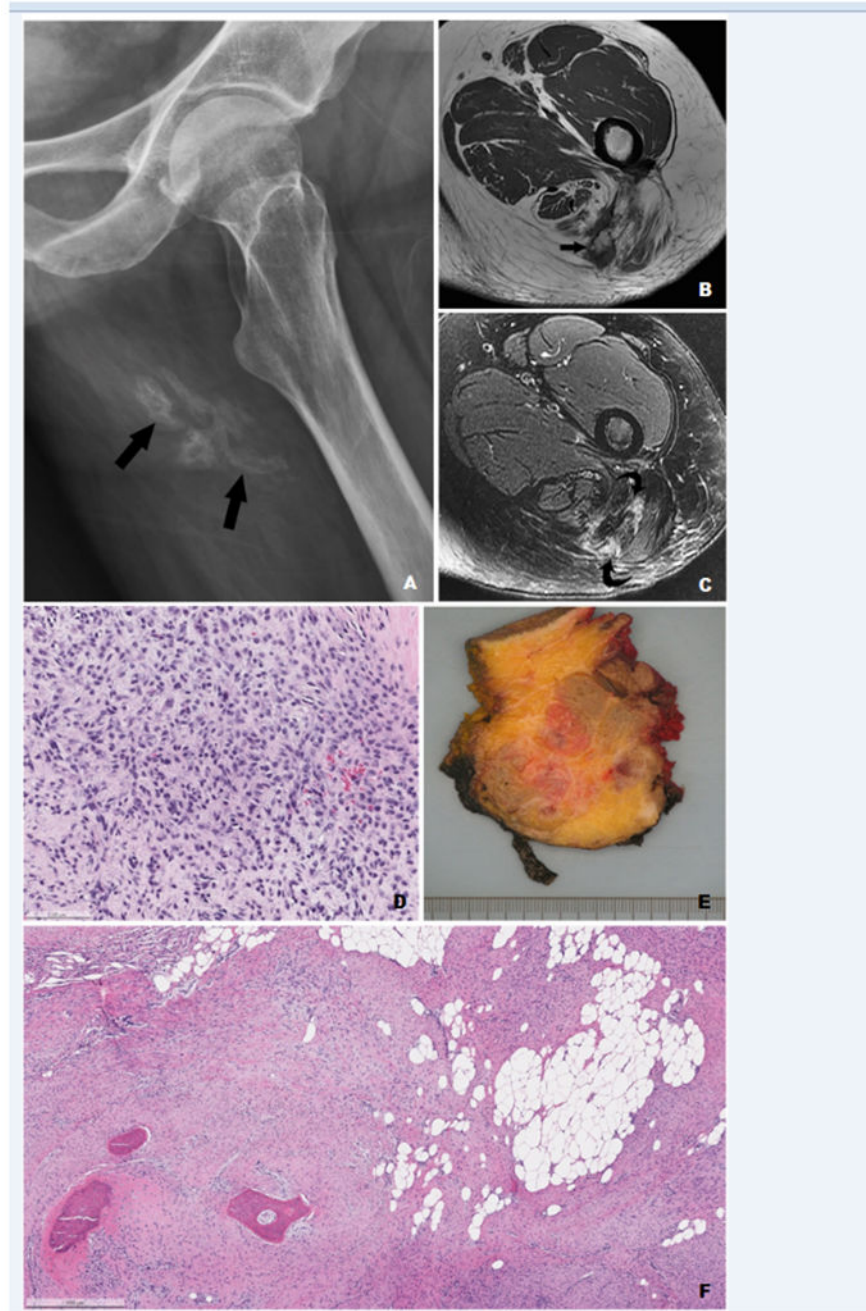
fibroblast-like spindle cells, osteoclast-like giant cells and background inflammatory cells, resembling primary ABC of bone.

Author Manuscript

Author Manuscript

Author Manuscript

Author Manuscript

**FIGURE 3.**

Case 3 - (A) A lateral radiograph showed a mass with clustered peripheral calcification (arrows) in the left proximal posterior thigh. **(B)** Axial T1-weighted and **(C)** T2-weighted MR image showed a mass infiltrating the gluteus maximus and hamstring muscles. The mass consisted of an ossified component (arrow) and a non-ossified soft tissue component (curved arrows). **(D)** A needle biopsy showed solid fibroblastic spindle cell proliferation in a collagenized stroma. **(E)** Gross examination showed an ill-defined and lobulated mass with multifocal ossification involving the deep adipose tissue and skeletal muscle. **(F)** Both

ossified and non-ossified components were present on histologic examination. In contrast to other cases with a zonal pattern, the non-ossified component composed of spindle cells infiltrated the adipose tissue with multiple haphazard foci of woven bone.

Author Manuscript

Author Manuscript

Author Manuscript

Author Manuscript

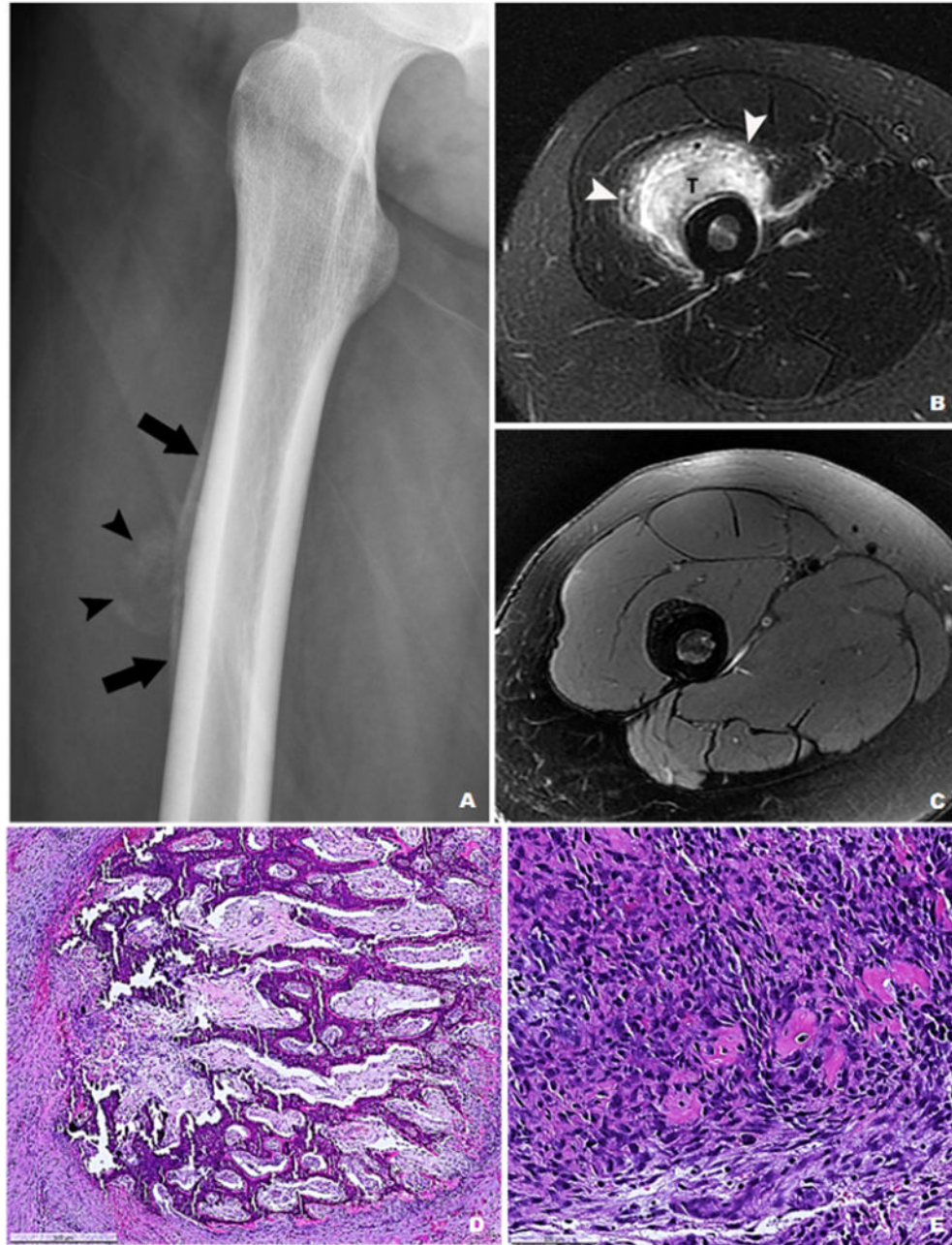


FIGURE 4.

Case 6 – (A) A radiograph showed a juxta-cortical mass with calcifications (arrowheads) and periosteal reaction (arrows). **(B)** On axial MRI STIR image, the mass (T) was surrounded by edema (arrowheads) and thickened soft tissue in the vastus intermedius muscle. No fluid level was identified. **(C)** Axial T2-weighted fat-suppressed image of the follow-up MRI 10 months after the open biopsy showed unchanged thick periosteal reaction along the femoral cortex with almost complete resolution of the previously identified high T2 signal, consistent with continued internal healing. **(D)** An incisional biopsy showed

exuberant interconnecting woven bone formation and (E) neighboring areas of fibroblastic proliferation with small foci of osteoid matrix.

Author Manuscript

Author Manuscript

Author Manuscript

Author Manuscript

Table 1. Summary of the Clinical, Radiological, and Pathological Features of Myositis Ossificans-like Soft Tissue Aneurysmal Bone Cyst

Patient	Age (years) / Sex	Site (size in cm)	Imaging findings	Pathology findings	FISH for <i>USP6</i> rearrangement	Fusion partner by targeted RNA sequencing	Treatment	Clinical Outcome
1	32/F	Thigh, subcutaneous tissue (4.0)	Ultrasound: Oval, partially cystic mass with mild peripheral vascular flow; Plain radiograph: (-) Calcification; MRI: Mass with thickened rim compressing and infiltrating the fascia, (+) perilesional edema, (+) fluid-fluid levels	Classic MO-like zonation with an ossified rim and central cystic spaces	Positive	<i>COL1A1</i> (exon 1)- <i>USP6</i> (exon 1)	Wide resection	Disease-free at 40 months
2	17/M	Supraclavicular soft tissue, juxta-cortical (2.3)	CT: Mass with (+) peripheral calcification contiguous with periosteal reaction at the sternocleidomastoid insertion; MRI: (+) Perilesional edema, (+) fluid-fluid levels	Classic MO-like zonation with an ossified rim and central cystic spaces	Positive	<i>COL1A1</i> (exon 1)- <i>USP6</i> (exon 1)	Wide resection	Disease-free at 5 months
3	46/F	Gluteal region, intra-muscular (7.5)	Ultrasound: Solid mass with (+) multifocal calcifications Plain radiograph: Multiple clustered calcifications, increased on post-biopsy studies; MRI: (+) Perilesional edema, (-) fluid-fluid levels	Ill-defined, fat-infiltrating fibroblasts with multifocal ossifications	Positive	<i>ANGPTL2</i> (exon 1)- <i>USP6</i> (exon 1)	Wide resection	Mass increased in size and symptoms persisted for 38 months prior to resection
4	51/F	Hypothear soft tissue (2.4)	Plain radiograph: Calcifications (-) at baseline but formed in 2 months; MRI: Lesion with diffuse low T1 and T2 signals and contrast enhancement, (+) extensive surrounding edema and soft tissue thickening, (-) fluid-fluid level	An evolving MO-like lesion with vague zonation, solid	Positive	<i>COL1A1</i> (exon 1)- <i>USP6</i> (exon 1)	En-bloc excision	Lost to follow-up
5	22/F	Axilla deep soft tissue (4.7)	Plain radiograph and CT: Mass with (+) peripherally calcified mass, increased on post-biopsy studies; MRI: Mass displacing the brachial plexus and axillary vessels without definitive infiltration, (+) perilesional edema, (+) fluid-fluid levels	Elements of a classic MO on biopsy, including blood-filled sinusoids	Positive	<i>COL1A1</i> (exon 1)- <i>USP6</i> (exon 1)	Incisional biopsy	Asymptomatic at 55 months
6	14/F	Thigh, juxta-cortical (2.9)	Plain radiograph and CT: Lesion with (+) peripheral and internal amorphous calcification, with associated periosteal reaction, increased on post-biopsy studies; MRI: Enhancing lesion in the vastus intermedius muscle, (+) perilesional edema, resolved subsequently, (-) fluid-fluid levels Bone scan: Intense radiotracer uptake, resolved on follow-up studies	Elements of classic MO on biopsy, solid	Positive	<i>COL1A1</i> (exon 1)- <i>USP6</i> (exon 1)	Incisional biopsy	Asymptomatic at 16 months
7	42/M	Thigh, intra-muscular	Ultrasound: Hypoechoic solid mass beneath the superficial fascia; Plain radiograph: Peripherally calcified	Elements of classic MO on biopsy, including small	Negative (limited cells analyzed)	<i>COL1A1</i> (exon 1)- <i>USP6</i> (exon 1)	Needle biopsy	Asymptomatic at 3 months

Patient	Age (years) / Sex	Site (size in cm)	Imaging findings	Pathology findings	FISH for <i>USP6</i> rearrangement	Fusion partner by targeted RNA sequencing	Treatment	Clinical Outcome
			mass, increased on post-biopsy radiographs; MRI: Diffusely enhancing mass with no neurovascular involvement, (+) perilesional edema, resolved subsequently and (-) fluid-fluid levels	blood-filled sinusoids				

Table 2.

Literature Review of Soft Tissue Aneurysmal Bone Cyst

Authors and year	Number of cases	Patient demographics and tumor location	Treatment and f/u information	Molecular analyses
Amir et al., 1992 ²⁰	1	15/F, groin	Excised with no recurrence	NP
Rodríguez-Peralto et al., 1994 ²¹	1	20/F, shoulder	N/A	NP
López-Barea et al., 1995 ²²	1	57/F, upper arm	Excised with no recurrence	NP
Shannon et al., 1997 ²³	1	29/F, retro-clavicular	Excised with no recurrence	NP
Nielsen et al., 2002 ²⁴	5	8/M, shoulder; 29/F, groin; 37/F, upper arm; 28/M, upper arm; 30/F, thigh	Excised with no recurrence	8/M, shoulder-t(17;17)(p13;q12) COL1A1-USP6 fusion ⁵
Wang et al., 2004 ²⁵	1	21/M, gluteus	Excised with no recurrence	NP
Ajillogba et al., 2005 ²⁶	1	12/F, thigh	Excised with no recurrence	NP
Ellison et al., 2007 ²⁷	1	10/F, thigh	Excised with no recurrence	t(5;17)(q33;p13)
Sukov et al., 2008 ¹⁰	2	11/M, thigh; 36/F, thigh	N/A	Both showed USP6 rearrangement
Pretchmann et al., 2011 ²⁸	2	26/F, thigh; 38/M, upper arm	Excised with no recurrence	Both showed USP6 rearrangement
Hao et al., 2012 ²⁹	1	10/F, shoulder	Excised with no recurrence	NP
Baker et al., 2015 ³⁰	1	41/F, upper arm	Excised with no recurrence	NP
Jacquot et al., 2015 ³¹	1	46/F, thigh	Excised with no recurrence	t(17;17)(p13;q21) COL1A1-USP6 fusion
Bekers et al., 2018 ¹¹	11	24/F, perineum; 19/F, leg; 28/M, arm; 44/M, thoracic wall; 25/M, thigh; 17/F, thigh; 38/F, thigh; 32/F, thigh; 8/F, knee; 56/M, thigh; 6/F, gluteus	N/A	8/11 cases showed USP6 rearrangement; 1/11 showed no USP6 rearrangement; 2/11 N/A
Švajdler et al., 2019 ¹²	15	44/M, thigh; 22/F, thigh; 28/M, gluteus; 35/F, thigh; 53/M, scapula; 10/M, neck; 35/M, thigh; 52/F, thigh; 19/F, arm; 31/M, thigh; 46/F, thigh; 37/F, arm; 60/M, thigh; 62/M, arm; 6/M, abdominal wall	N/A	5/15 showed COL1A1-USP6 fusion; 2/15 showed no USP6 rearrangement on sequencing; 8/15 N/A
Song et al., 2019 ¹³	6	49/F, thigh; 34/F, thigh; 15/M, thigh; 19/F, thigh; 16/F, abdominal wall; 32/M, gluteus	Excised with no recurrence	3/6 cases showed COL1A1-USP6 fusion; 1 additional case showed USP6 rearrangement; 2/6 cases failed FISH and RNA sequencing studies
Our series	7	32/F, thigh; 17/M, supraclavicular soft tissue; 46/F, gluteus; 51/F, hand; 22/F, axilla; 14/F, thigh; 41/M, thigh	3/7 excised with no recurrence; 3/7 clinical stable on f/u; 1/7 lost to f/u	6/7 cases showed COL1A1-USP6 fusion; 1/7 case showed ANGPTL2-USP6 fusion

Abbreviations: N/A = Not available; NP = Not performed; f/u = follow-up

Table 3.

Neoplasms with *USP6* rearrangement

Entity	Pathological features	5' partner genes to <i>USP6</i>	Comment
STABC (MO-like STABC)	Circumscribed or infiltrative lesion in the skeletal muscle or associated with fascia. Most cases have MO-like histologic features with zonal growth pattern, with dynamic change over time; Early reports commonly described ABC-like cystic spaces, but solid cases have also been reported	<i>COL1A1</i> , <i>ANGPTL2</i>	Overlapping clinical and pathological features and growing molecular evidence suggest they are closely related entities; however, the literature on the frequency of <i>USP6</i> gene rearrangement in MO is contradictory (17%, ¹⁰ to 89% ¹¹)
Classic MO and Fibro-osseous pseudotumor of digits	Circumscribed lesion in the skeletal muscle; Early (<6 weeks) lesion is cellular, composed of oval to spindle fibroblastic/osteoblastic cells in a loose collagenous to myxoid stroma. More mature lesions have a classic zonal growth pattern, with reactive woven bone forms at the periphery; Erythrocyte extravasation and osteoclast-like giant cells may or may not be evident	<i>COL1A1</i> ^{11,12,38} (few cases)	
ABC of bone	Primary lytic and expansile bone lesion with multiloculated blood-filled cystic spaces separated by fibrous septa; The fibrous septa contain cellular proliferation of fibroblastic spindle cells, osteoclast-like giant cells and reactive woven bone rimmed by osteoblasts; Solid variant lacks cystic spaces	<i>CDH11</i> , <i>CNBP</i> , <i>CTNNB1</i> , <i>E1F1</i> , <i>STAT3</i> , <i>COL1A1</i> , <i>PAPAH1B1</i> , <i>THRAP3</i> , <i>FOSL2</i> , <i>SEC31A</i> , <i>SPARC</i> , <i>RUNX2</i> , <i>OMD</i> and <i>USP9X</i> ⁵⁻⁹	Giant cell rich lesion of the small bones ("Giant cell reparative granulomas of bone" in hands and feet) harbor <i>USP6</i> rearrangement ³⁵ <i>USP6</i> rearrangement is not present in secondary ABC in association with benign and malignant bone tumors ⁴
Nodular fasciitis	Circumscribed or infiltrative lesion in the subcutaneous tissue, composed of plump fibroblastic spindle cells in a myxoid to collagenized stroma with a tissue culture-like growth pattern; erythrocyte extravasation and osteoclast-like giant cells may or may not be evident.	<i>MYH9</i> , <i>RRBP1</i> , <i>CALU</i> , <i>CTNNB1</i> , <i>MIR22HG</i> , <i>SPARC</i> , <i>THBS2</i> , and <i>COL6A2</i> ^{32,33}	<i>MYH9</i> , <i>SPARC</i> , <i>SERP1NH1</i> , and <i>COL3A1</i> have been identified as partner genes to <i>USP6</i> in cranial fasciitis ³⁷
Cellular fibroma of tendon sheath	Increased cellularity compared to classic fibroma of tendon sheath, composed of loosely formed fascicles of spindled-to-stellate fibroblasts with areas of microcystic change and erythrocyte extravasation	Unrevealed ³⁴	

Abbreviations: ABC – aneurysmal bone cyst; STABC – soft tissue aneurysmal bone cyst; MO – myositis ossificans